Construction and Optimization of Power Transfer Route in Array Wireless Power Transfer Network With Multiple Load Nodes

Jinde Wu, Zhuohang Jin, Xiaoxia Han, Wenjie Zhang, Qintao Zhao, and Zuotong Liang

***Abstract*—Wireless power transfer network (WPTN) is composed of nodes and power transfer routes, which can supply power for group devices. In the application of WPTN, the number and position of load nodes are usually random. The random variation and the adjustment of output characteristics of some load nodes will affect the electrical performance of the other nodes due to the complex cross-coupling. This article constructs an array WPTN that can maintain the independence of the node output current with the load change by designing a special topology structure. Combined with the topology structure switching strategy of nodes, the power transfer direction can be flexibly adjusted according to the position of load nodes. On this basis, the power transfer routes are optimized for the goal of maximum efficiency. And the breadth-first search algorithm is adopted to optimize the power transfer routes based on its fast search speed. Finally, the experimental results verify the effectiveness of the proposed method.**

***Index Terms*—Multiple load nodes, power transfer route optimization, wireless power transfer network (WPTN).**

NOMENCLATURE

Symbol	*Description*
U_{dc0}	Input dc voltage of power source node.
U_{ac0}	Output ac voltage RMS of power source node inverter.
f, ω	Operating frequency and angular frequency.
L_{i1}, L_{i2}	Self-induction of coils in each node.
R_{Li1}, R_{Li2}	Equivalent ac series resistances of coil.
C_{i1}, C_{i2}, and C_{i3}	Resonant capacitance of each node.
$M_{i1\_(i+1)1}$, $M_{i1\_(i+1)2}$ $M_{i2\_(i+1)1}$, $M_{i2\_(i+1)2}$	Mutual inductance between adjacent node coils.
R_i, R_{li}	Load impedance and equivalent ac impedance.
C_i	Filter capacitor of each node.
U_{out_ij}	Output voltage of the node in row i and column j.

Manuscript received 29 August 2023; revised 9 November 2023; accepted 2 December 2023. Date of publication 6 December 2023; date of current version 26 January 2024. This work was supported by the Fundamental Research Program of Shanxi Province under Grant 202203021212209. Recommended for publication by Associate Editor J. Acero. *(Corresponding author: Jinde Wu.)*

The authors are with the School of Electrical and Power Engineering, Taiyuan University of Technology, Taiyuan 030024, China (e-mail: wujinde@tyut.edu.cn; jinzhuohang0409@link.tyut.edu.cn; hanxiaoxia@tyut.edu.cn; zhangwenjie@tyut.edu.cn; zhaoqintao0410@link.tyut.edu.cn; 2023510367@link.tyut.edu.cn).

Color versions of one or more figures in this article are available at https://doi.org/10.1109/TPEL.2023.3339974.

Digital Object Identifier 10.1109/TPEL.2023.3339974

I. INTRODUCTION

IN THE wireless power transfer network (WPTN), it is difficult to build determined power transfer routes and ensure stable power supply for each node because of the complex cross coupling among devices. If load-independent output voltage or current for multiple loads can be satisfied, and combined with the construction and optimization method of power transfer route, it will improve the performance of WPTN.

There are some relevant papers about wireless power transfer through the repeaters. Generally, in the previous studies, the repeaters can be added between the transmitter and the receiver to increase the transmission distance [1], enhance the transfer power and efficiency [2], and improve the system performance [3]. *LCC* topology is used in paper [4], and constant voltage outputs can be obtained for all the loads, which facilitates the independent load power control. In order to maintain constant transfer power and keep near-unity transfer efficiency at varying transfer distances, paper [5] proposes a WPT system with multiple repeaters based on the concept of parity-time symmetry. In addition to achieving constant output power, the transfer efficiency can be against the variation of the transfer distance without any tuning or feedback within a certain distance. The mathematical expression for the power transfer efficiency with an optimal load is derived in paper [6] to improve the power transfer efficiency, and it also analyzes the effects of the varying repeater numbers on the power transfer efficiency. It confirms that there is an optimal repeater number for maximizing the achievable power transfer efficiency for a given end-to-end distance. Paper [7] proposes a bidirectional multistage wireless power transfer method for robot arm that can provide energy for multiple loads. A bowl-coupling structure and three-dimensional orthogonal ring coil are proposed to reduce coupling variation against joint rotation. With a special resonant topology design for each stage, energy can be injected or output freely on each stage regardless of energy transfer direction. This topology can also reduce the sensitivity of the output voltages with the variation of the loads. Paper [8] proposes an optimal design for mid-range WPT system based on multiple repeaters.

The optimized spaced structure with different distances is investigated to further optimize the system, which can improve the transfer efficiency under the same distance requirement. Paper [9] proposes a modular-stacked multiport wireless energy interconnection system with a virtual ac bus for multisource and multiload WPT applications, which can realize the flexible regulation of the power flow. Paper [10] proposes a methodology for the design of WPT resonators that can achieve optimum efficiency for multiple receivers with power distribution ratios, loads, and distances. The system includes multiple repeaters, and each of them is connected to a resistive load. Each receiver transfers power to an adjacent receiver and acts as a relay while its local load consumes power. A 2.5 m five-stage WPT system based on domino cylindrical solenoid coupler, and compensated respectively in layers, is proposed in paper [11]. The system is considered to be used as 220 kV post insulators application, transferring power for sensors and measuring instruments of smart grids. With the same application in paper [11], the system proposed in paper [12] can realize constant voltage and constant current by adjusting the receiver's switch state. The domino WPT system proposed in paper [13] also can achieve constant current output. Moreover, the system efficiency can be further improved by optimizing the number of coils and layers under the condition that the transfer distance is fixed. The method of graph sets is proposed in paper [14] to model, analyze, and simplify the multicoil WPT system, and a set of rules are developed to analyze some important aspects. The above research works mainly focus on system performance improvement by adding multiple repeaters. However, due to that each node role is preset, so power transfer route across multiple nodes is normally fixed and cannot be changed dynamically. Therefore, the above repeaters-working modes cannot support the WPTN operations, which will limit WPT technology applications for group electronic devices.

There are some relevant papers about WPT system with multiple receivers. Paper [15] proposes a WPT system with dual transmitters and dual receivers as well as integrated decoupling coils is introduced. Besides mitigating the mutual inductances of the same-side coils, the proposed decoupling coils are also taking part in power transfer. Paper [16] proposes a free-positioning omnidirectional WPT system with a reticulated planar transmitter, which enables multiple receivers to be powered simultaneously in arbitrary positions and orientations. Paper [17] describes a comparative study of the frequency-selective WPT by considering two different configurations, Tx–Rx–Rx and Rx–Tx–Rx, in a multiple-receiver system. In this system, the receivers have different resonant frequencies and a transmitter can select a driving frequency to transfer power. The system proposed in paper [18] can also transfer power with different resonant frequencies to multiple receivers simultaneously. Compared with the typical multiple-frequency and multiple-receiver WPT system, the proposed WPT system can reduce considerable amount of power switches. Paper [19] proposes and implements an autonomous current compensation scheme, which can be taken as an impedance buffer to ensure the resonant state for the expected operating frequency. The proposed scheme allows for an enhanced exciting current of the primary coil and transfers power in multiple-pickup WPT system. The above research works mainly focus on transferring power to multiple receivers. However, due to the complex cross coupling among nodes in WPTN, it is difficult to transfer power to multiple receivers simultaneously.

Breadth-first search algorithm has been widely used in some fields. Some references on breadth-first search algorithm are as follows. A new algorithm that searches the optimal lattice points by lattice theory through the breadth-first algorithm is described in paper [20]. This algorithm reduces the ambiguity search space by calculating and judging the Euclidean distance between each search variable and the target one so as to improve the search efficiency. Paper [21] proposes a reliable routing algorithm that combines the improved breadth-first search and a graph neural network. The proposed algorithm can effectively alleviate network congestion, improve throughput, and reduce end-to-end delay and packet loss rate. In paper [22], the problem of determining all reducts of an information system is formulated as a graph search problem. The proposed algorithm uses a breadth-first search strategy to search for all reducts starting from the graph root. It expands nodes in breadth-first order and uses a pruning rule to decrease the search space. The proposed algorithm is both time and space efficient. Paper [23] presents three heuristic algorithms for reliability estimation based on breadth-first search of a grid tree. The conclusion indicates that the use of breadth-first search can significantly reduce redundant samplings.

In order to satisfy power transfer among array WPTN, this article proposes a power transfer route construction and optimization method considering complex cross coupling. The power transfer route can be changed dynamically according to different node power requirements, and the node role can be changed accordingly by using topology switching method. This method increases the flexibility in group device charging and helps to set up a more reliable wireless power route to extend effective wireless power transfer area. Furthermore, load-independent output current for multiple loads can be achieved to improve the stability of the system. Combined with the breadth-first search algorithm, the optimal power transfer route can be quickly constructed.

II. Array Wireless Power Transfer Network

There are several potential applications of array WPTN. One of the applications is in the robot field. In modern mines, dangerous gas detection robots have been widely used. Due to the influence of gas, it is prohibited to charge the robots by wired connection in the underground. The usual practice is to charge the robots after they are lifted on the ground, which takes a lot of time, and the process is very complicated. The method of wireless charging is considered to solve this problem. However, due to the narrow and complex space underground, it is difficult to set a sufficiently large transmitting coil to charge all robots. Therefore, multiple robots can be designed to form the array WPTN as shown in Fig. 1. The power can be transferred through the routes among the devices.

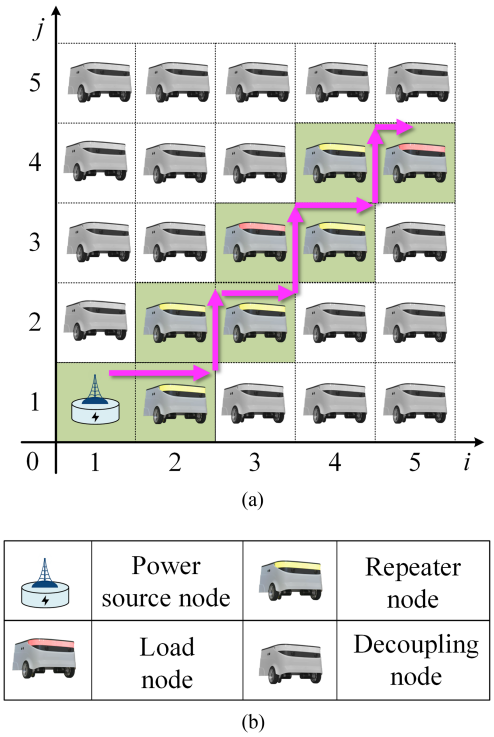

Fig. 1. Array wireless power transfer network and node roles. (a) Array wireless power transfer network. (b) Node roles.

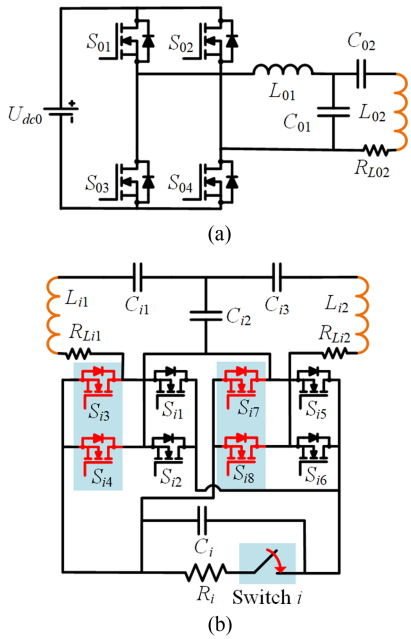

Fig. 2. Circuit models of different nodes. (a) Power source node. (b) Other nodes.

In order to satisfy different power transfer requirements, the nodes can be divided as power source node, repeater node, load node, and decoupling node.

1) Power source node provides power source for WPTN.
2) Repeater node extends the area of WPTN and does not consume power.
3) Load node actually consumes power.
4) Decoupling node does not participate in the power transfer.

The circuit models of different nodes are designed in Fig. 2. To analyze the system, some basic definitions are given as follows. As can be seen in Fig. 2(a), the power source node is composed of a power supply ($U_{\rm dc0}$), a full-bridge inverter (S_{01}–S_{04}), and a resonance compensation network (L_{01}–C_{01}–C_{02}–L_{02}). Other nodes shown in Fig. 2(b) are composed of a resonance compensation network (L_{i1}–C_{i1}–C_{i2}–C_{i3}–L_{i2}), two full-bridge converters (S_{i1}–S_{i4} and S_{i5}–S_{i8}), a switch (Switch i), a filter capacitor (C_i), and a load (R_i). The coil resistances are expressed as R_{Li1} and R_{Li2}, and the equivalent ac impedance of the Load node before the rectifier is expressed as R_{li}. The operation frequency of the inverter on Power source node is f, and its angular frequency is ω ($\omega = 2\pi f$).

The relation between the dc voltage $U_{\rm dc0}$ and inverter output voltage $U_{\rm ac0}$ is as follows:

$$U_{\rm ac0} = \frac{2\sqrt{2}U_{\rm dc0}}{\pi}. \tag{1}$$

In the designed topology, when the capacitances and inductances of each node satisfy (2), the equivalent impedances of each node exhibit resistive

$$\begin{cases} \omega^2 = \frac{1}{L_{01}C_{01}} = \frac{1}{L_iC_{i2}} \\ j\omega L_{01} = j\omega L_{02} + \frac{1}{j\omega C_{02}} \\ j\omega L_{i1} + \frac{1}{j\omega C_{i1}} \\ \quad = j\omega L_{i2} + \frac{1}{j\omega C_{i3}} = j\omega L_i \end{cases} \quad (i = 1, 2 \ldots). \tag{2}$$

In order to achieve different objectives of power transfer, each node can switch its role according to different power transfer routes. This article proposes a topology switching method to change the role of nodes, and the topology model is shown in Fig. 2(b). Node-simplified circuit model and node role under different converter states are shown in Table I.

III. Independence Analysis of Node Output Current About Load Change and the Design of Coupling Mechanism

A. Independence Analysis of Node Output Current About Load Change

In the WPTN with multiple load nodes, if the node output voltage or current is independent of the load, the stability of the system will be improved. The node designed in this article includes two coils, one of which receives the power from the previous node and transfers the power to the next node through the other coil. Due to the randomness of the node position and the complexity of cross-coupling between nodes, the selection of the coil role (transmitting or receiving) on the node needs to be determined according to the mutual inductance between nodes. On this basis, if the load can be controlled to be connected in series to the branch of the transmitting coil, and the sensitivity of the transmitting coil current to the load variation can be reduced,

TABLE I
NODE SIMPLIFIED CIRCUIT MODEL AND ROLE UNDER DIFFERENT STATES

Converter state	Simplified circuit model	Node role
S_{i3}/S_{i4}: ON S_{i7}/S_{i8}: Rectification Switch i: ON	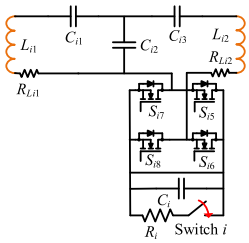	Load node (The load is serially connected to C_{i3}–L_{i2}–R_{Li2} branch)
S_{i3}/S_{i4}: Rectification S_{i7}/S_{i8}: ON Switch i: ON	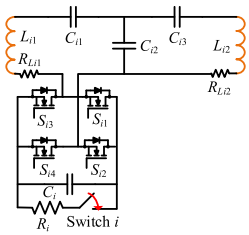	Load node (The load is serially connected to L_{i1}–C_{i1}–R_{Li1} branch)
S_{i3}/S_{i4}: ON S_{i7}/S_{i8}: ON Switch i: ON	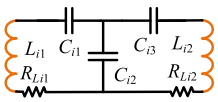	Repeater node
S_{i3}/S_{i4}: OFF S_{i7}/S_{i8}: OFF Switch i: OFF	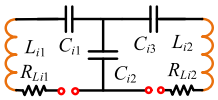	Decoupling node

TABLE II
EXPERIMENTAL PARAMETERS

Parameter	Value	Parameter	Value
U_{dc0}	40 V	f	150 kHz
L_{01}	5 μH	C_{01}	225 nF
L_{02}	85 μH	C_{02}	14 nF
L_{i1}	85 μH	L_{i2}	85 μH
C_{i1}	14 nF	C_{i3}	14 nF
C_{i2}	225 nF	R_{Li1}	0.05 Ω
R_{Li2}	0.05 Ω	R_i	10 Ω

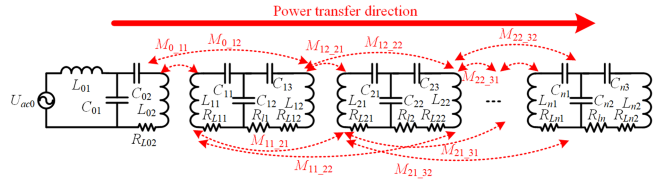

Fig. 3. Coupling relationship of nodes on the constructed power transfer route.

it will verify that the output current of each node is independent of the load.

Fig. 3 shows the coupling relationship between nodes when the power is transmitted in a certain direction in the built power transfer route. In the power transfer link, when two nodes are separated from the other nodes, the mutual inductance between them is usually ignored because of the long distance. Therefore, only the mutual inductance between adjacent nodes needs to be considered.

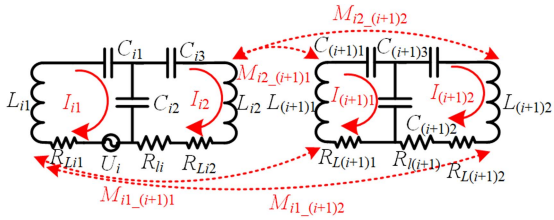

Fig. 4. Coupling relationship between two nodes under cross-coupling condition.

It is complex to analyze the node output performance under the condition of the WPTN with multiple load nodes. Taking full account of the cross-coupling between coils, we take two nodes as the example to analyze the factors those affect the output current of nodes and extend it to the applications of multiple nodes.

The coupling relationship between two nodes under cross-coupling condition is shown in Fig. 4, and the load is connected in series with L_{i2} and $L_{(i+1)2}$, respectively. When the capacitance and inductance in each node satisfy (2), the KVL equation is listed as follows:

$$\begin{cases} \dot{U}_i = R_{Li1}\dot{I}_{i1} - \frac{1}{j\omega C_{i2}}\dot{I}_{i2} + j\omega M_{i1\_(i+1)1}\dot{I}_{(i+1)1} \\ \qquad +j\omega M_{i1\_(i+1)2}\dot{I}_{(i+1)2} \\ 0 = -\frac{1}{j\omega C_{i2}}\dot{I}_{i1} + (R_{Li2} + R_{li})\,\dot{I}_{i2} + j\omega M_{i2\_(i+1)1} \\ \dot{I}_{(i+1)1} + j\omega M_{i2\_(i+1)2}\dot{I}_{(i+1)2} \\ 0 = j\omega M_{i1\_(i+1)1}\dot{I}_{i1} + j\omega M_{i2\_(i+1)1}\dot{I}_{i2} + R_{L(i+1)1} \\ \dot{I}_{(i+1)1} - \frac{1}{j\omega C_{(i+1)2}}\dot{I}_{(i+1)2} \\ 0 = j\omega M_{i1\_(i+1)2}\dot{I}_{i1} + j\omega M_{i2\_(i+1)2}\dot{I}_{i2} - \frac{1}{j\omega C_{(i+1)2}} \\ \dot{I}_{(i+1)1} + \left(R_{L(i+1)2} + R_{l(i+1)}\right)\dot{I}_{(i+1)2}. \end{cases} \quad (3)$$

Since the coil resistance is very small compared with the load impedance, in order to facilitate calculation, it is assumed that the coil resistance is ignored, that is, $R_{Li1} = 0$, $R_{Li2} = 0$, $R_{L(i+1)1} = 0$, and $R_{L(i+1)2} = 0$. According to (3), load current I_{i2} and $I_{(i+1)2}$ can be expressed as follows: (4) shown at the bottom of the next page, where, A, B, C, D, and E are as follows:

$$\begin{cases} A = \omega C_{(i+1)2} R_{l(i+1)} M_{i1\_(i+1)1} M_{i2\_(i+1)1} \\ B = C_{(i+1)2} M_{i1\_(i+1)1}^2 R_{li} R_{l(i+1)} \omega/2 \\ C = M_{i1\_(i+1)1} M_{i1\_(i+1)2} R_{li} \\ D = M_{i1\_(i+1)1} R_{li} \\ E = M_{i1\_(i+1)1} M_{i2\_(i+1)2} + M_{i1\_(i+1)2} M_{i2\_(i+1)1}. \end{cases} \quad (5)$$

According to (4) and (5), if $M_{i1\_(i+1)1} = 0$, I_{i2} and $I_{(i+1)2}$ can be expressed as follows:

$$\begin{cases} \lim\limits_{M_{i1\_(i+1)1}\to 0} \dot{I}_{i2} = \\ \dfrac{j\dot{U}_i C_{i2}\omega\left(C_{i2}C_{(i+1)2}M_{i1\_(i+1)2}M_{i2\_(i+1)1}\omega^4 - 1\right)}{\left(C_{i2}C_{(i+1)2}M_{i1\_(i+1)2}M_{i2\_(i+1)1}\omega^4 - 1\right)^2} \\ \lim\limits_{M_{i1\_(i+1)1}\to 0} \dot{I}_{(i+1)2} = \\ \dfrac{j\dot{U}_i C_{i2} C_{(i+1)2} M_{i2\_(i+1)1}\omega^3\left(C_{i2}C_{(i+1)2}M_{i1\_(i+1)2}M_{i2\_(i+1)1}\omega^4 - 1\right)}{\left(C_{i2}C_{(i+1)2}M_{i1\_(i+1)2}M_{i2\_(i+1)1}\omega^4 - 1\right)^2}. \end{cases} \quad (6)$$

Fig. 5. Orthogonal coupling mechanism model.

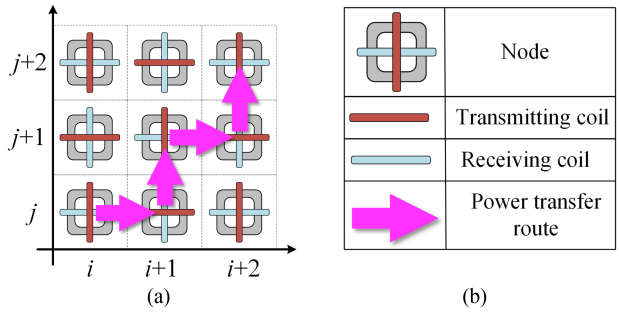

Fig. 6. Rules for power transfer in array WPTN. (a) 3 × 3 array wireless power transfer subnetwork and power transfer route. (b) Marking of coils and power transfer route.

When (6) satisfies (7), I_{i2} and $I_{(i+1)2}$ can be expressed as (8)

$$C_{i2}C_{(i+1)2}M_{i1\_(i+1)2}M_{i2\_(i+1)1}\omega^4 - 1 \neq 0 \tag{7}$$

$$\begin{cases} \lim\limits_{M_{i1\_(i+1)1}\to 0} \dot{I}_{i2} = \dfrac{j\dot{U}_i C_{i2}\omega}{C_{i2}C_{(i+1)2}M_{i1\_(i+1)2}M_{i2\_(i+1)1}\omega^4 - 1} \\ \lim\limits_{M_{i1\_(i+1)1}\to 0} \dot{I}_{(i+1)2} = \dfrac{j\dot{U}_i C_{i2}C_{(i+1)2}M_{i2\_(i+1)1}\omega^3}{C_{i2}C_{(i+1)2}M_{i1\_(i+1)2}M_{i2\_(i+1)1}\omega^4 - 1}. \end{cases} \tag{8}$$

It can be seen from (8) that I_{i2} and $I_{(i+1)2}$ are independent of the load under above conditions. Therefore, the limiting conditions for the output current independent of the load are as follows.

1) $M_{i1\_(i+1)1}\to 0$, that is, the mutual inductance between the receiving coils of two adjacent nodes is close to 0.
2) $C_{i2}C_{(i+1)2}M_{i1\_(i+1)2}M_{i2\_(i+1)1}\omega^4 - 1 \neq 0$.

The relationship between I_{i2} and $I_{(i+1)2}$ is as follows:

$$I_{(i+1)2} = \frac{M_{i2\_(i+1)1}}{L_i} I_i. \tag{9}$$

According to the above analysis, under the condition that the current of the transmitting coils on two nodes is constant, stable induction voltage and constant transmitting coil current can be provided for the next node. In addition, this limitation condition can also be extended to the case of multiple nodes.

B. Design of Coupling Mechanism

Based on the above independence analysis of node output current about load change, the orthogonal coupling mechanism model as shown in Fig. 5 is designed to ensure that the mutual inductance between the two coils is 0.

IV. Construction and Optimization of Power Transfer Route

A. Construction of Power Transfer Route

According to the above theoretical analysis, the mutual inductance between receiving coils of adjacent nodes should be reduced. Therefore, when WPTN is applied to array electrical device, nodes need to be arranged according to certain rules.

A 3 × 3 array wireless power transfer subnetwork with nine nodes ($N_{(i,\ j)}$, $N_{(i+1,\ j)}$, $N_{(i+2,\ j)}$, $N_{(i,\ j+1)}$, $N_{(i+1,\ j+1)}$, $N_{(i+2,\ j+1)}$, $N_{(i,\ j+2)}$, $N_{(i+1,\ j+2)}$, and $N_{(i+2,\ j+2)}$) is shown in Fig. 6(a). Each node includes two mutually orthogonal coils (transmitting coil and receiving coil) those are marked in Fig. 6(b). According to the direction of power flow from $N_{(i,\ j)}$ to $N_{(i+2,\ j+2)}$) in Fig. 6(a), a pair of coils parallel to each other in adjacent nodes is used as the transmitting coil of the previous node and the receiving coil of the next node. It can be seen that under this node arrangement and coil selection mode, the receiving coils of adjacent nodes are naturally perpendicular to each other, and the mutual inductance between them is very small, even approaching 0. It meets the condition that each node transmitting coil current, that is, the load current is independent of the load. Furthermore, the power cannot continuously pass through two nodes in the direction of horizontal or vertical. The power is transferred from the power source node to other nodes following the rule of horizontal or vertical alternation, and it is shown in Fig. 6(a).

In the array WPTN, the number and position of load nodes are random. Therefore, there are multiple routes to traverse all load nodes from the power source node, and the coil role needs to be changed adaptively according to the direction of the power flow, and then the power transfer route will also increase with the increase of the number of nodes. Therefore, this article will optimize the power transfer route for the goal of efficiency optimization.

$$\begin{cases} \dot{I}_{i2} = -\dfrac{\omega\dot{U}_i C_{i2}\left(-j + C_{(i+1)2}\omega^4(-A+jE)C_{i2}\right)}{-1+2C_{(i+1)2}\omega^5\left(-C_{(i+1)2}E^2\omega^3/2 - B + jC\right)C_{i2}^2 + 2C_{(i+1)2}(jA+E)\omega^4 C_{i2}} \\ \dot{I}_{(i+1)2} = -\dfrac{C_{(i+1)2}\omega^3\dot{U}_i\left(\left(jC_{(i+1)2}M_{i2\_(i+1)1}\omega^3 E - D\right)\omega C_{i2} + jM_{i2\_(i+1)1}\right)C_{i2}}{-1+2C_{(i+1)2}\omega^5\left(-C_{(i+1)2}E^2\omega^3/2 - B + jC\right)C_{i2}^2 + 2C_{(i+1)2}(jA+E)\omega^4 C_{i2}} \end{cases} \tag{4}$$

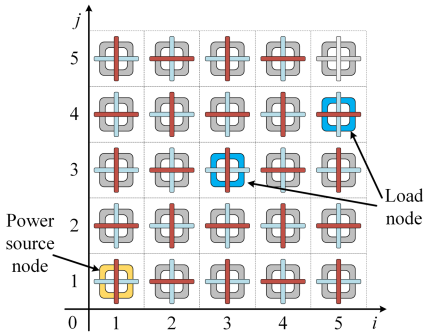

Fig. 7. 5 × 5 array WPTN.

B. Optimization Objective of Power Transfer Route

In the research of WPT system, efficiency and power are the main indicators to evaluate the system. In the array WPTN, power needs to be transferred from power source node to all load nodes through the repeater nodes, and other unrelated nodes need to be decoupled. The efficiency of the system can be expressed as follows:

$$\eta = \frac{\sum P_{\text{out\_}i}}{P_{\text{in}}}. \tag{10}$$

In (10), $\Sigma P_{\text{out\_}i}$ is the total output power of all load nodes, and P_{in} is the input power. In the WPT system, the loss caused by the coil resistances (R_{Li1} and R_{Li2}) is mainly considered. Therefore, the total loss P_{loss} can be expressed as follows:

$$P_{\text{loss}} = \sum I_{Li1}^2 R_{Li1} + \sum I_{Li2}^2 R_{Li2} = P_{r\_\text{loss}} + P_{t\_\text{loss}}. \tag{11}$$

In (11), I_{Li1} and I_{Li2} are the currents of the receiving coil and transmitting coil of all load nodes and repeater nodes respectively, and P_{r_loss} and P_{t_loss} are the total losses of them, respectively. According to the above analysis, the power needs to be transferred from the power source node to each load node through adjacent node one by one. Therefore, fewer repeater nodes mean smaller total loss and higher efficiency, so that the issue of building the optimal power transfer route will be adjusted to find the route with the minimum number of total repeater nodes. Therefore, the optimization objective of power transfer route can be described as follows.

1) Meeting the power demand of all load nodes.
2) Minimum total number of repeater nodes.

C. Optimization of Power Transfer Route

A 5×5 array WPTN is taken as an example to describe the power transfer route optimization method. It can be seen from Fig. 7 that N_{11} is the power source node, N_{33} and N_{54} are load nodes. The power should be transferred from N_{11} to N_{33} and N_{54} with the minimum number of total repeater nodes, and it is also defined as the shortest power transfer route.

First, we will describe the growth method of node input tree and output tree, and the shortest power transfer route between different nodes. According to the power transfer rule

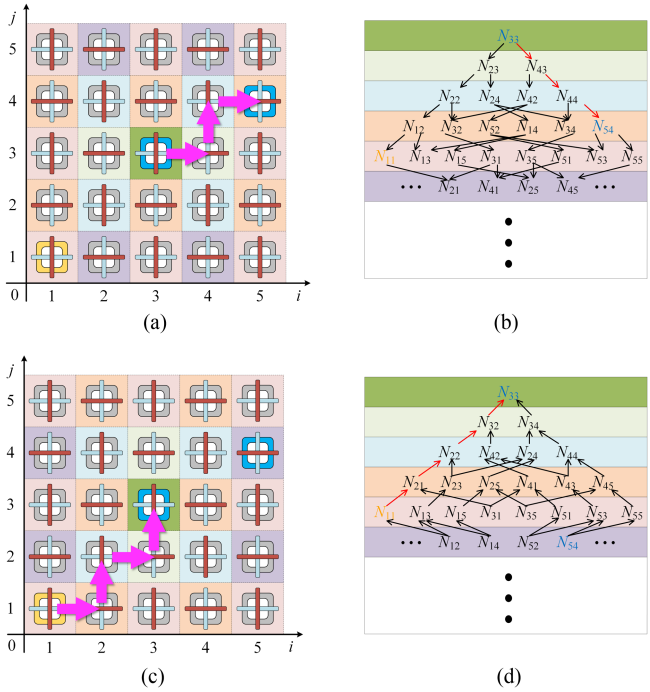

Fig. 8. Growth method of N_{33} input tree and output tree based on breadth-first search algorithm. The (a) input layer and (b) input tree of N_{33}, the (c) output layer and (d) output tree of N_{33}.

and breadth-first search algorithm, N_{33} is selected as the root node to grow the input tree and output tree step by step, and it is shown in Fig. 8(b) and (d). Obviously, because the tree structure is generated by breadth-first traversal, for the input tree and the output tree, the fewer number of nodes on the branch, the shorter the corresponding power transfer route. Such as the shortest power transfer route from N_{33} to N_{54} is $N_{33}\rightarrow N_{43}\rightarrow N_{44}\rightarrow N_{54}$, and the shortest power transfer route from N_{11} to N_{33} is $N_{11}\rightarrow N_{21}\rightarrow N_{22}\rightarrow N_{32}\rightarrow N_{33}$. Furthermore, they are marked by the lines of red arrows in Fig. 8(b) and (d), and the corresponding routes are marked in Fig. 8(a) and (c).

The input tree and output tree of different load nodes (N_{33} and N_{54}) are grown as shown in Fig. 9(b). If the input tree of a load node and the output tree of another load node have the same nodes, these same nodes are defined as key nodes (N_{43} and N_{44}). Then, the trees are merged as shown in Fig. 9(b) and the load nodes are combined with the key nodes to construct a subnetwork (N_{33}, N_{54}, N_{43}, and N_{44}) as shown in Fig. 9(c). The same as node, the input tree and output tree of the subnetwork are grown until all the load nodes and the power source node are included in the network, and it is shown in Fig. 9(d). Finally, the shortest power transfer route should be constructed according to the method shown in Fig. 8, and it is the optimal power transfer route.

The flowchart of power transfer route optimization is shown in Fig. 10, and the optimal power transfer route is shown in Fig. 11.

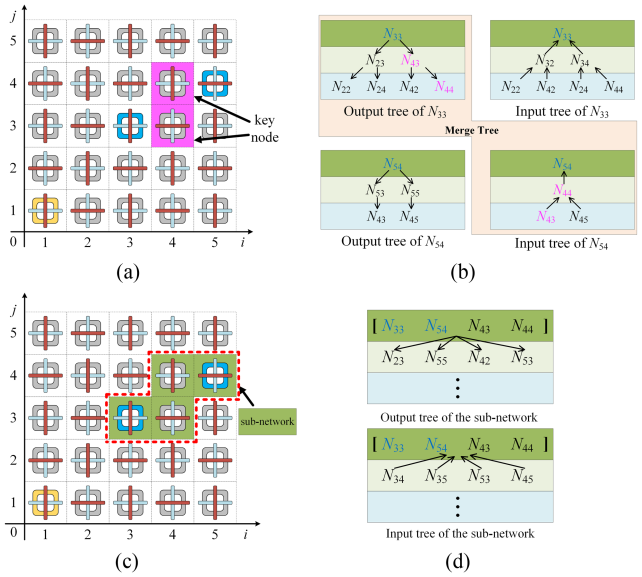

Fig. 9. Merging trees and constructing subnetwork. (a) Marking key nodes. (b) Finding the key nodes and merging trees. (c) Constructing subnetwork. (d) Constructing input and output trees for subnetworks.

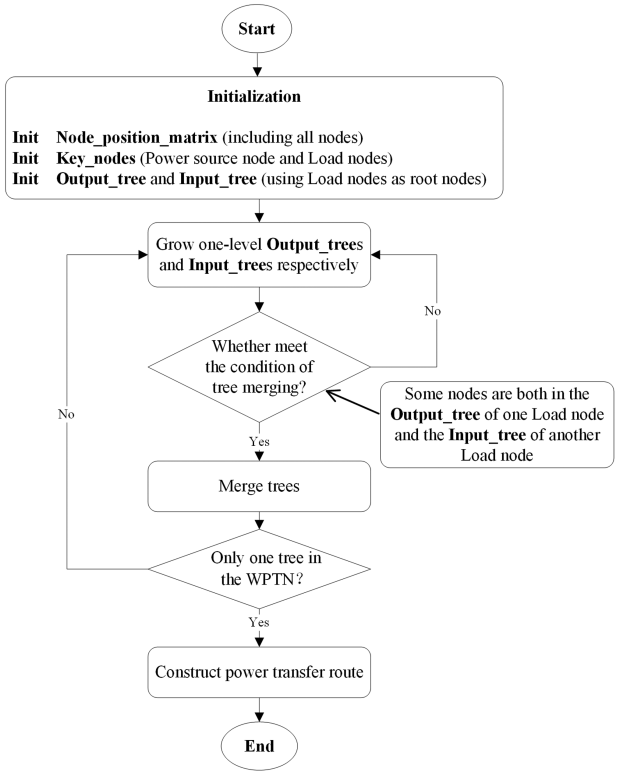

Fig. 10. Flowchart of power transfer route optimization.

V. Experimental Verification

In order to verify the proposed method, an experimental platform shown in Fig. 12 is set up. The system consists of a 3 × 3 array wireless power transfer network with nine nodes, and the nodes are marked as N_{11}, N_{12}, N_{13}, N_{21}, N_{22}, N_{23}, N_{31}, N_{32}, and N_{33}. Each node consists of two orthogonally

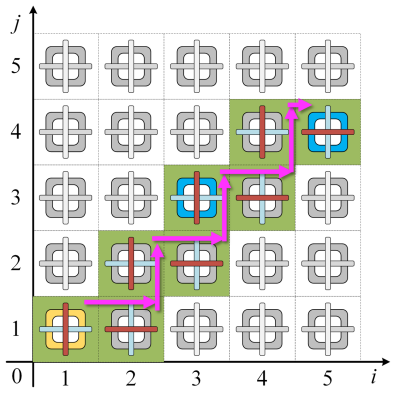

Fig. 11. Optimal power transfer route.

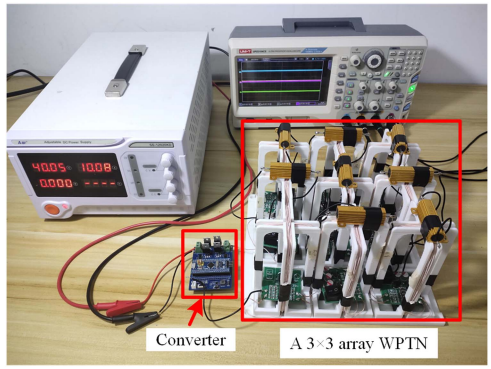

Fig. 12. Experimental platform.

distributed coils. The topology of the nodes is designed as shown in Fig. 2. The experimental parameters are shown in Table II. In the designed array WPTN, each node is designed to be approximately the same, including inductances, capacitances, and mutual inductances between adjacent nodes.

Under the condition of cross coupling between nodes, it is very important to maintain the stability and independence of each node. It can be seen from Fig. 13 that when N_{33}, N_{23}, N_{22}, and N_{12} are decoupled in turn, the output voltage of each load node remains almost unchanged. Therefore, the output voltage of each node can be adjusted independently. This enhances the stability and flexibility of output voltage regulation. Furthermore, according to (9), if $L_i = M_{i2\_(i+1)1}$ is set in the parameter design of the node topology structure, then the capacitance of the capacitor is designed according to (1). The current of the transmitting coils on the nodes those are in the power transfer route will be approximately equal, which means that the output voltage U_{out_i} on the load nodes will be approximately equal. It can be seen from Fig. 13 that the output voltages of each load node are approximately equal, where $U_{\mathrm{out}\_12} = 19.2$ V, $U_{\mathrm{out}\_22} = 18.5$ V, $U_{out\_32} = 18.2$ V, and $U_{\mathrm{out}\_33} = 17.9$ V. The output voltages are approximately equal, which can reduce the difficulty of output voltage regulation. Furthermore, the efficiencies on different power transfer routes are shown in Fig. 13, and they are 70.2%, 77.36%, 81.28%, and 83.08%, respectively.

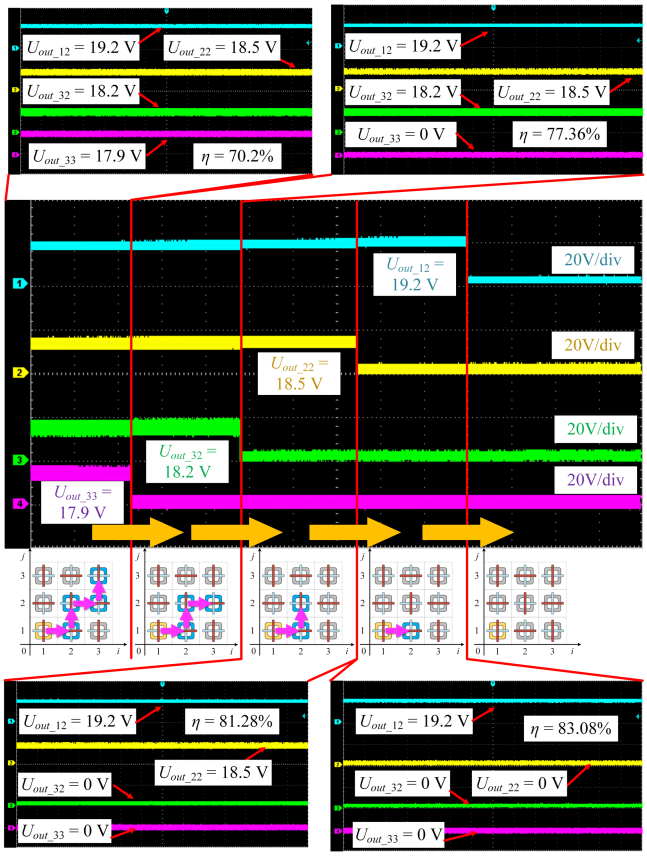

Fig. 13. Dynamic node role switching.

VI. Conclusion

This article proposes a power transfer route construction and optimization method for array WPTN. With the topology structure switching strategy of node, the power transfer route and the node role can be switched dynamically. Besides, under the condition of considering cross coupling, and analyzing the relationship between nodes, the limiting conditions of node output current and load independence are obtained. This enhances the stability of the system. Furthermore, based on the breadth-first search algorithm, the power transfer route has been optimized to ensure that the power is transmitted from the power source node to all load nodes with the minimum number of total repeater nodes, thereby achieving optimal efficiency. Finally, a 3 × 3 array WPTN verifies the stability of system operation under the condition of dynamic node role switching. In addition, according to the relationship between the current of the transmitting coil of the adjacent nodes, the output voltages of each node can be approximately equal by designing the parameters of the node topology, which can reduce the difficulty of output voltage regulation.

References

[1] F. Zhang, S. A. Hackworth, W. Fu, C. Li, Z. Mao, and M. Sun, "Relay effect of wireless power transfer using strongly coupled magnetic resonances," *IEEE Trans. Magn.*, vol. 47, no. 5, pp. 1478–1481, May 2011.

[2] S. Y. R. Hui, W. Zhong, and C. K. Lee, "A critical review of recent progress in mid-range wireless power transfer," *IEEE Trans. Power Electron.*, vol. 29, no. 9, pp. 4500–4511, Sep. 2014.

[3] C. K. Lee, W. X. Zhong, and S. Y. R. Hui, "Effects of magnetic coupling of nonadjacent resonators on wireless power domino-resonator systems," *IEEE Trans. Power Electron.*, vol. 27, no. 4, pp. 1905–1916, Apr. 2012.

[4] C. Cheng, W. Li, Z. Zhou, Z. Deng, and C. Mi, "A load-independent wireless power transfer system with multiple constant voltage outputs," *IEEE Trans. Power Electron.*, vol. 35, no. 4, pp. 3328–3331, Apr. 2020.

[5] X. Shu, B. Zhang, Z. Wei, C. Rong, and S. Sun, "Extended-distance wireless power transfer system with constant output power and transfer efficiency based on parity-time-symmetric principle," *IEEE Trans. Power Electron.*, vol. 36, no. 8, pp. 8861–8871, Aug. 2021.

[6] J. Lee and K. Lee, "Effects of number of relays on achievable efficiency of magnetic resonant wireless power transfer," *IEEE Trans. Power Electron.*, vol. 35, no. 7, pp. 6697–6700, Jul. 2020.

[7] J. Wu, X. Dai, R. Gao, and J. Jiang, "A coupling mechanism with multidegree freedom for bidirectional multistage WPT system," *IEEE Trans. Power Electron.*, vol. 36, no. 2, pp. 1376–1387, Feb. 2021.

[8] Y. Guan, Y. Xiao, Y. Cui, and D. Xu, "Analysis and optimal design of mid-range WPT system based on multiple repeaters," *IEEE Trans. Ind. Appl.*, vol. 58, no. 1, pp. 1092–1100, Jan./Feb. 2022.

[9] M. Zhou, F. Liu, K. Lu, and X. Chen, "Modular stacked multiport wireless energy interconnection system with virtual AC bus and its power flow control strategy," *IEEE Trans. Power Electron.*, vol. 37, no. 12, pp. 15774–15784, Dec. 2022.

[10] J.-H. Cho, S. Jung, and Y.-J. Kim, "Wireless power transfer for variable load- distance- and power division ratio in a loosely-coupled multiple-receiver relay system," *IEEE Trans. Ind. Electron.*, vol. 70, no. 7, pp. 6809–6818, Jul. 2023.

[11] P. Gu et al., "A 2.5m long-range IPT system based on domino cylindrical solenoid coupler compensated respectively in layers," *IEEE Trans. Ind. Electron.*, vol. 70, no. 2, pp. 1409–1420, Feb. 2023.

[12] Z. Yan et al., "A monitoring equipment charging system for HVTL based on domino-resonator WPT with constant current or constant voltage output," *IEEE Trans. Power Electron.*, vol. 37, no. 3, pp. 3668–3680, Mar. 2022.

[13] Z. Dong, S. Liu, X. Li, Z. Xu, and L. Yang, "A novel long-distance wireless power transfer system with constant current output based on domino-resonator," *IEEE J. Emerg. Sel. Topic Power Electron.*, vol. 9, no. 2, pp. 2343–2355, Apr. 2021.

[14] F. Faradjizadeh, D. M. Vilathgamuwa, P. Jayathurathnage, and G. Ledwich, "Graph sets method for multicoil wireless power transfer systems—Part I: Principles," *IEEE Trans. Power Electron.*, vol. 35, no. 10, pp. 10741–10756, Oct. 2020.

[15] A. Hossain, P. Darvish, S. Mekhilef, K. S. Tey, and C. W. Tong, "A new coil structure of dual transmitters and dual receivers with integrated decoupling coils for increasing power transfer and misalignment tolerance of wireless EV charging system," *IEEE Trans. Ind. Electron.*, vol. 69, no. 8, pp. 7869–7878, Aug. 2022.

[16] T. Feng, Z. Zuo, Y. Sun, X. Dai, X. Wu, and L. Zhu, "A reticulated planar transmitter using a three-dimensional rotating magnetic field for free-positioning omnidirectional wireless power transfer," *IEEE Trans. Power Electron.*, vol. 37, no. 8, pp. 9999–10015, Aug. 2022.

[17] K. Lee and S. H. Chae, "Comparative analysis of frequency-selective wireless power transfer for multiple-rx systems," *IEEE Trans. Power Electron.*, vol. 35, no. 5, pp. 5122–5231, May 2020.

[18] Y. Xiao, C. Liu, Y. Huang, and S. Liu, "Concurrent wireless power transfer to multiple receivers with additional resonant frequencies and reduced power switches," *IEEE Trans. Ind. Electron.*, vol. 67, no. 11, pp. 9292–9301, Nov. 2020.

[19] Z. Zhang, H. Pang, S. H. K. Eder, and R. Kennel, "Self-balancing virtual impedance for multiple-pickup wireless power transfer," *IEEE Trans. Power Electron.*, vol. 36, no. 1, pp. 958–967, Jan. 2021.

[20] S. Wang et al., "A partial ambiguity resolution algorithm based on new-breadth-first lattice search in high-dimension situations," *Sensors*, vol. 22, no. 19, pp. 1–13, Oct. 2022.

[21] P. Lu, C. Jing, and X. Zhu, "GraphSAGE-based multi-path reliable routing algorithm for wireless mesh networks," *Processes*, vol. 11, no. 4, pp. 1–19, Apr. 2023.

[22] V. Boonjing and P. Chanvarasuth, "Efficient breadth-first reduct search," *Mathematics*, vol. 8, no. 5, pp. 1–12, May 2020.

[23] X. Chen et al., "Heuristic algorithms for reliability estimation based on breadth-first search of a grid tree," *Rel. Eng. System Saf.*, vol. 232, pp. 1–19, Jan. 2023.

Jinde Wu received the B.S. degree in automation from the College of Information Engineering, Taiyuan University of Technology, Taiyuan, China, in 2015, and the Ph.D. degree in control theory and control engineering from the School of Automation, Chongqing University, Chongqing, China, in 2021.

He is currently working with the College of Electrical and Power Engineering, Taiyuan University of Technology. His main research interests include wireless power transfer, computer vision, and intelligent sensor and detection technology.

Zhuohang Jin received the B.S. degree in electrical engineering and automation from the College of Electromechanical Engineering, Hainan University, China, in 2020. He is currently working toward the master's degree in control science and engineering in the Taiyuan University of Technology, Taiyuan, China.

His current research interests include wireless power transfer and power electronics.

Xiaoxia Han received the M.A.Sc. degree in control theory and engineering and the Ph.D. degree in circuits and systems from the Taiyuan University of Technology, Taiyuan, China, in 2005 and 2010, respectively.

From 2015 to 2016, she was a Visiting Scholar with the University of Saskatchewan, Canada. She has been a Professor with the Taiyuan University of Technology, since 2019. She has authored more than 40 articles. Her research interests include modeling and optimal control of complex industrial process, machine learning and intelligent computing, intelligent sensor, detection technology, and wireless power transfer.

Wenjie Zhang received the B.S. degree in energy engineering and automation from the North China University of Technology, Beijing, China, in 2016, and the Ph.D. degree in electrical engineering from the Institute of Electrical Engineering, Chinese Academy of Sciences, Beijing, China, in 2022.

He is currently working with the College of Electrical and Power Engineering, Taiyuan University of Technology, Taiyuan, China. His main research interests include battery management system, wireless power transfer, and artificial intelligence.

Qintao Zhao received the B.S. degree in automation from the Taiyuan Institute of Technology, Taiyuan, China, in 2021, where he is currently working toward the master's degree in control engineering.

His current research interests include wireless power transfer and power electronics.

Zuotong Liang received the B.S. degree in automation from the College of Electrical and Power Engineering, Taiyuan University of Technology, Taiyuan, China, in 2023, where he is currently working toward the master's degree in control science and engineering.

His current research interests include wireless power transfer and power electronics.